

# Green Synthesis, Surface Activity, Micellar Aggregation, and Foam Properties of Amide Quaternary Ammonium Surfactants

Xinru Jia, Ran Wei, Bo Xu, Hongqin Liu,\* and Bao-Cai Xu

Cite This: *ACS Omega* 2022, 7, 48240–48249

Read Online

ACCESS |



Metrics &amp; More

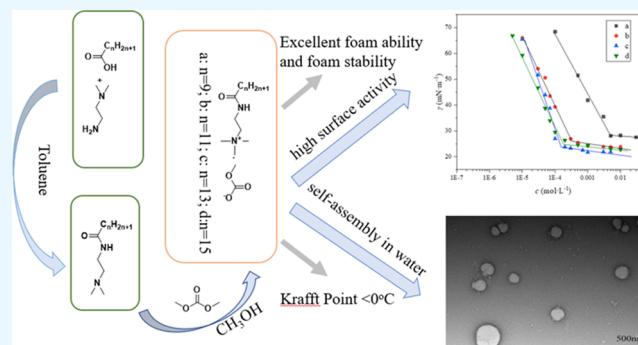


Article Recommendations



Supporting Information

**ABSTRACT:** A series of amide quaternary ammonium surfactants with the formula  $C_nH_{2n+1}CONH(CH_2)_2N^+(CH_3)_3\cdot CH_3CO_3^-$  ( $n = 9, 11, 13, 15$ ) were synthesized using a fatty acid, *N,N*-dimethylethylenediamine, and a green reagent dimethyl carbonate. A comparative study of the four surfactants in terms of surface activity, aggregation characteristics, and foam properties was conducted. The results show that these amide quaternary ammonium surfactants reduce the surface tension of water to a minimum value of  $23.69 \text{ mN}\cdot\text{m}^{-1}$  at a concentration of  $1.55 \times 10^{-4} \text{ mol}\cdot\text{L}^{-1}$  and self-assemble spontaneously into aggregates, which are mostly vesicles. Furthermore, with increasing the alkyl chain length, their critical micelle concentration (CMC) values and surface tension values at the CMC ( $\gamma_{CMC}$ ) decrease and then increase, and the degree of counterion binding ( $\beta$ ) decreases. It is also found that these amide quaternary ammonium surfactants exhibit excellent foam ability and foam stability.



## 1. INTRODUCTION

Quaternary ammonium cationic surfactants have attracted more and more attention due to their excellent properties, such as the ability to reduce surface tension, allowing to enhance the wettability of the interface and surface, low toxicity, a wide range of biological activities, chemical stability, and good solubility in water.<sup>1–6</sup> As emulsifiers, bactericides, detergents, antistatic agents, fabric softeners, phase transfer catalysts, corrosion inhibitors, dispersants, wetting agents, foaming agents, etc., they are widely used in various fields of life, such as agriculture, medicine, biotechnology, food industry, and so on.<sup>1,2</sup> Quaternary ammonium cationic surfactants also play an important role in the development of high technology and the preparation of nano and intelligent materials.<sup>7</sup>

However, most of the surfactants used are nondegradable in nature, and their use have caused serious water pollution and environmental safety problems.<sup>8,9</sup> It has been reported that the biodegradability of surfactants can be improved by introducing various cleavable groups such as ester, amide, carbonate, etc., which are susceptible to chemical/enzymatic hydrolysis, into surfactant molecules.<sup>9,10</sup> In addition, it was also found that the insertion of amide groups into surfactant molecules would lead to significant changes in their surface activity and micellization.<sup>10–12</sup> The study of Hoque et al. showed that the amide functionality increases the surfactant aggregation tendencies compared to the surfactants without an amide bond, and the aggregation properties of the gemini surfactants containing amide groups are closely related to the position and number of amide bonds.<sup>10</sup>

At present, most of the methylating agents for the synthesis of quaternary ammonium surfactants are methyl halides ( $CH_3X$ ,  $X = I, Br, Cl$ ) and dimethyl sulfate, which are toxic and corrosive chemicals.<sup>9,13–17</sup> In addition, the reaction usually requires a stoichiometric amount of alkali and produces some inorganic salts that need to be treated. Dimethyl carbonate (DMC) is a well-known nontoxic reagent and an environmentally benign substitute for methyl halides and dimethyl sulfate.<sup>18–20</sup> Moreover, the reaction, using DMC as the methylation reagent, does not produce inorganic salts, and the leaving group methyl carbonate decomposes to produce only methanol and  $CO_2$  as byproducts.<sup>18</sup> With the increasingly serious environmental problems, the concepts of green chemistry, sustainable development, and environmental protection have been paid more and more attention.<sup>21</sup> DMC, as a “green” methylating reagent, incorporates several of these fundamental aspects of green chemistry, such as avoiding the use of toxic and dangerous chemicals, being more atom-efficient, and so on. Herein, to develop safe, efficient, and environmentally friendly surfactants, a new series of quaternary ammonium surfactants containing amide bonds are synthe-

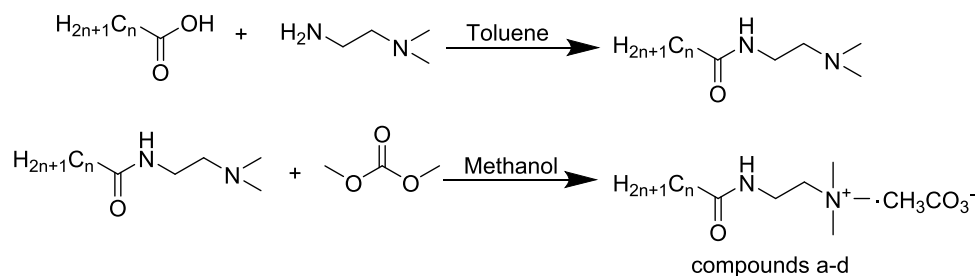
Received: October 1, 2022

Accepted: December 7, 2022

Published: December 15, 2022



## Scheme 1. Synthesis of Alkyl Amide Ethyl Trimethyl Ammonium Carbonate (Compounds a–d)



compound a: n=9; compound b: n=11; compound c: n=13; compound d: n=15

sized using DMC as the methylating reagent. Their surface activity, microstructure, and aggregation properties are studied. Their foam properties are also determined.

## 2. EXPERIMENTAL METHODS

**2.1. Materials.** *N*-Decanoic acid (99%), lauric acid (98%), myristic acid (99%), palmitic acid (97%), *N,N*-dimethylethylenediamine (98%), dimethyl carbonate (99%), and sodium lauryl benzene sulfonate (LAS, 95%) were analytical pure and purchased from Shanghai Maclean Biochemical Technology Co., Ltd. Toluene (99.5%) and anhydrous methanol (99.5%) were analytical pure and provided by Sinopharm Chemical Reagent Beijing Co., Ltd. The high-purity water ( $\rho = 18.25 \text{ M}\Omega\cdot\text{cm}^{-1}$ ) was supplied by a Milli-Q ultrapure water purification system.

**2.2. Synthesis of Alkyl Amide Ethyl Trimethyl Ammonium Carbonate.** These amide quaternary ammonium surfactants are prepared via a two-step synthetic route, which is shown in Scheme 1.

First, 0.1 mol *N,N*-dimethylethylenediamine and 0.15 mol fatty acid (*N*-decanoic acid, lauric acid, myristic acid, palmitic acid) were added to a 250 mL round-bottomed flask equipped with a magnetic stirrer, then an appropriate amount of toluene as a solvent was added. The reaction mixture was heated at 125 °C with agitation for 5 h and then cooled to room temperature. After the reaction, the solvent toluene was removed by rotary evaporation to obtain the light yellow paste solid alkyl amide ethyl dimethyl tertiary amine. Alkyl amide ethyl dimethyl tertiary amine (0.05 mol), DMC (0.25 mol), and an appropriate amount of methanol as a solvent were added to a 500 mL stainless steel autoclave reactor. The reaction mixture was stirred for 8 h at 423.15 K and 1.4 MPa. After the reaction, methanol and the excess DMC were removed by vacuum rotary evaporation. Then, the products were extracted in the water layer through a two-phase extraction with water and ethyl acetate. Finally, water was removed by lyophilization to give the pure brown powder product alkyl amide ethyl trimethyl ammonium carbonate (compounds a–d).

**2.3. Structure Characterization.** Mass spectrometry (MS) analysis was performed using an AB SCIEX API3200 liquid chromatography tandem mass spectrometer.  $^1\text{H}$  NMR and  $^{13}\text{C}$  NMR spectra were obtained on a Bruker AVANCEIII HD proton nuclear magnetic resonance spectrometer with  $\text{CD}_3\text{OD}$  and  $\text{DMSO}-d_6$  as solvents. Fourier transform infrared (FTIR) spectra were recorded on a Nicolet is 10 infrared spectrometer.

**2.4. Krafft Temperature Determination.** The aqueous solutions of these amide quaternary ammonium surfactants with a mass fraction of 1% (above the CMC) were prepared

respectively and then were heated under stirring until they were clear and transparent. After that, the aqueous solutions of these surfactants were cooled on an ice–water bath until there was solid precipitation, and the corresponding temperature, namely, Krafft point, was recorded. All of the above experiments were repeated three times. In addition, Krafft temperature was also measured by the conductivity method. The prepared 1% surfactant aqueous solutions were kept in a refrigerator for 10 h at about 0 °C. Then, the conductivity of these surfactant aqueous solutions was measured via a DDS-307 conductivity meter (cell constant:  $0.997 \text{ cm}^{-1}$ ) with the temperature ranging from 0 to 20 °C. Each temperature gradient was measured three times.

**2.5. Surface Tension Measurements.** At 298.15 K, the surface tension of the amide quaternary ammonium surfactant aqueous solution was determined using the Delta8 surface tensiometer of Kibron, Finland, via the Wilhemy plate method within a concentration range of  $1 \times 10^{-7}$ – $1 \times 10^{-2} \text{ mol}\cdot\text{L}^{-1}$ . Three measurements were performed on each solution sample. Surface tension was an average of triplicate measurements, and the standard deviation was less than 0.02.

**2.6. Conductivity Measurement.** The conductivity of these surfactant aqueous solutions within a concentration range of  $1 \times 10^{-5}$ – $1 \times 10^{-2} \text{ mol}\cdot\text{L}^{-1}$  was measured using a DDS-307 conductivity meter at 298.15 K. Each sample was measured three times to determine the average value with the standard deviation less than  $0.016 \mu\text{S}\cdot\text{cm}^{-1}$ .

**2.7. Steady-State Fluorescence Measurements.** Using pyrene as a probe, a HITACHI F-4500 fluorescence spectrometer was used to determine the CMC and the aggregate micropolarity of the surfactants. Surfactant solutions within a concentration range of  $1 \times 10^{-6}$ – $0.1 \text{ mol}\cdot\text{L}^{-1}$  were prepared with a saturated aqueous solution of pyrene as the solvent, in which the concentration of pyrene was  $1 \times 10^{-6} \text{ mol}\cdot\text{L}^{-1}$ . The surfactant solutions were first vibrated by ultrasound for 1 h, then stored in 60 °C water bath for 2 h, and finally stored in 40 °C water bath overnight. The fluorescence emission spectra were measured at 298.15 K with the excitation wavelength of 335 nm, the excitation slit width of 5 nm, the emission slit width of 2.5 nm, the scanning wavelength of 350–450 nm, and the scan speed of  $60 \text{ nm}\cdot\text{min}^{-1}$ . The fluorescence intensities of the pyrene in peaks  $\lambda_1$  (372 nm) and  $\lambda_3$  (384 nm), i.e.,  $I_1$  and  $I_3$ , from the emission spectrum at each concentration, were recorded. According to the ratio of  $I_1/I_3$ , the CMC and the surfactant aggregate micropolarity were determined.

**2.8. Dynamic Light Scattering (DLS) Measurements.** DLS measurements were made using a Malvern Zetasizer Nano ZS instrument at 298.15 K with a solid-state He–Ne

laser as the light source (22 mW output power,  $\lambda = 632.8$  nm). The detection angle was  $173^\circ$ . The surfactant solution with a concentration of 5CMC was introduced into a light-transmitting cuvette through a  $0.45 \mu\text{m}$  filter membrane and then equilibrated for 3 min before measurements. Each solution sample was measured at least three times with a standard deviation of less than 0.002. The distribution of the solute diffusion coefficient ( $D$ ) was obtained based on analyzing the correlation function of scattering data via the CONTIN method. Then, the apparent equivalent hydrodynamic radius ( $R_h$ ) can be calculated according to the Stokes–Einstein equation  $R_h = kT/6\pi\eta D$ , where  $k$  is the Boltzmann constant,  $T$  is the absolute temperature, and  $\eta$  is the solvent viscosity.

**2.9. Transmission Electron Microscopy (TEM) Measurements.** TEM micrographs were obtained by the negative-staining method with 2% uranyl acetate solution as the staining agent. A drop of surfactant aqueous solution with the concentration of 5CMC was put on a clean sealing film; after that, the porous carbon support film (260 mesh) was inverted on the droplet for 6 min and then was dried in a vacuum dryer for at least 12 h. Subsequently, a drop of 2% uranyl acetate was put on another clean sealing film; then, the adsorbed carbon support film was inverted on the droplet and dyed for 35 s and then was dried in a vacuum dryer for at least 12 h. Finally, TEM images were recorded on an OXFORD X-MAX JEM-2100 electron microscope operating at an accelerating voltage of 120 kV.

**2.10. Foam Measurements.** The foam properties were determined using a foam scanner (FoamScan IT Concept, Teclis Co., Lyon, France) through the bubble method at 25, 35, and  $45^\circ\text{C}$ , respectively. Surfactant solutions ( $40 \text{ mL}$ ) with a concentration of  $0.01 \text{ mol}\cdot\text{L}^{-1}$  were injected into the instrument, and then,  $\text{N}_2$  was supplied at a gas flow rate of  $40 \text{ mL}\cdot\text{s}^{-1}$  to blow foam. The time required for the generated foam volume to reach  $130 \text{ mL}$  was used to express the foaming ability. The gas supply was stopped when the foam volume reached  $130 \text{ mL}$ . After  $1000 \text{ s}$ , the remaining foam volume was used to evaluate the foam stability. For comparison, the foam properties of LAS solutions at the same concentration were analyzed.

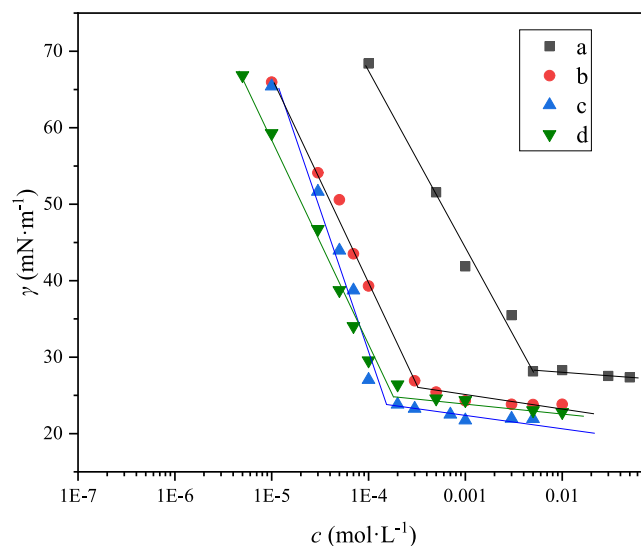
### 3. RESULTS AND DISCUSSION

**3.1. Synthesis and Characterization.** These synthesized amide quaternary ammonium surfactants were characterized by their MS,  $^1\text{H}$  NMR,  $^{13}\text{C}$  NMR, and FTIR spectra. For the details of these spectral characterizations, see the Supporting Information. In a word, the structures of all of these compounds are confirmed.

**3.2. Krafft Temperature.** The amide quaternary ammonium surfactant solution did not show any sign of precipitation after standing in an ice–water bath for 24 h. So, the Krafft temperatures for all of these amide quaternary ammonium surfactants are assigned to be below  $0^\circ\text{C}$ . In addition, the conductivity ( $\kappa$ ) versus temperature plots of these surfactant aqueous solutions are shown in Figure S18. The migration of counterions in salt-free systems will affect the conductivity value.<sup>22</sup> When the temperature rises to the Krafft point, the conductivity value increases sharply because the improvement of solubilities can increase counterion density. Therefore, the Krafft temperature can be determined by the turning points of the plot of the conductivity versus temperature. As seen from Figure S18, no turning points are observed owing to their low Krafft temperature ( $<0^\circ\text{C}$ ) over the examined temperature

range. So, it can be safely concluded that the Krafft temperature for these surfactants is below  $0^\circ\text{C}$ , which indicates that these surfactants have good water solubility. The amide linkage in the quaternary ammonium surfactant molecules can form a hydrogen bond with water molecules, which leads to a significant improvement of the solubility. The low Krafft temperature and good hydrophilicity make these amide quaternary ammonium surfactants have wide usage temperature range, broadening their fields of application.

**3.3. Surface Activity and Surface Property Parameters.** The surface tension ( $\gamma$ ) values of these amide quaternary ammonium surfactant aqueous solutions against the concentration ( $c$ ) are plotted in Figure 1. As is seen in Figure 1, the

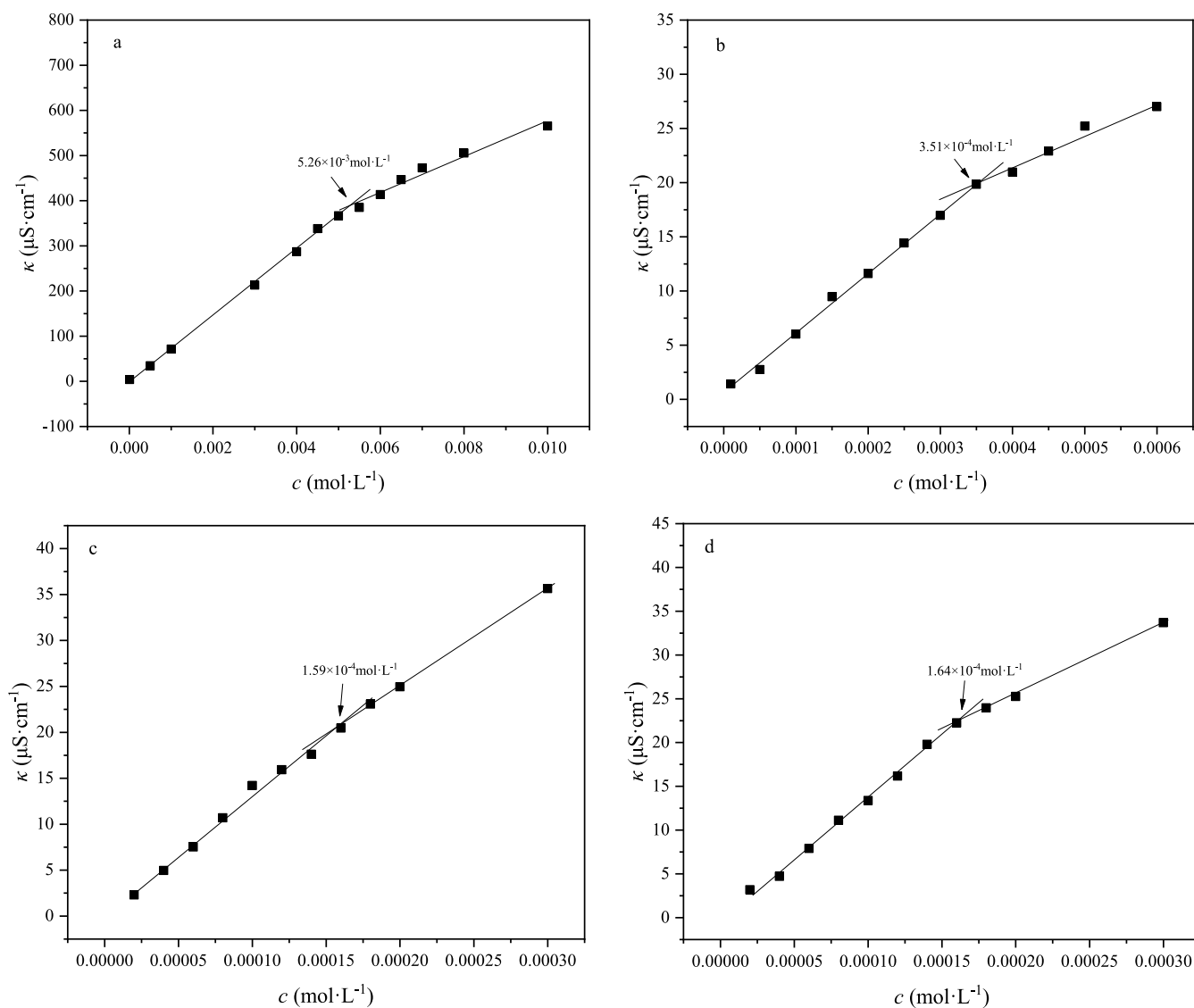


**Figure 1.** Plots of surface tension ( $\gamma$ ) versus the concentration ( $c$ ) of compounds a, b, c, and d at  $298.15 \text{ K}$ .

surface tension of aqueous solutions initially decreases with an increase in the concentration of these amide quaternary ammonium surfactants and then reaches a plateau, which means the formation of micelles. The CMC values are determined from the intersection point of the surface tension curve. The CMC values and the surface tension value at the CMC ( $\gamma_{\text{CMC}}$ ) are listed in Table 1. It can be found that the CMC values of these amide quaternary ammonium surfactants are  $1.55 \times 10^{-4}$ – $5.08 \times 10^{-3} \text{ mol}\cdot\text{L}^{-1}$ , lower than those of such typical cationic surfactants as alkyl trimethyl ammonium bromides and alkyl dimethyl ethyl ammonium bromides with the same alkyl chain length.<sup>23,24</sup> This may be because the presence of amide groups in these surfactants facilitates enhanced aggregation through intermolecular hydrogen bonding and the hydrophobic interaction<sup>10</sup> and also probably facilitates intermolecular association among surfactants through hydrogen bonding interactions in organized assemblies,<sup>11</sup> thus leading to the lower CMC. Another reason may be that the weak hydrophilicity of the  $\text{CH}_3\text{CO}_3^-$  counterion of these surfactants is conducive to micellization,<sup>25</sup> resulting in the lower CMC. Further, compared with the CMC values of some quaternary ammonium surfactants that have been reported,<sup>26,27</sup> these values are still lower, which demonstrates that the surface activities of these amide quaternary ammonium surfactants are superior, indicating an excellent micelle forming ability. In addition, as is seen in Table 1, the  $\gamma_{\text{CMC}}$  values of these surfactants are between 23.69 and  $28.08$

Table 1. Surface Active Properties and Parameters of the Micellization for compounds a, b, c, and d at 298.15 K

compound	CMC (mol·L <sup>-1</sup> )	$\gamma_{\text{CMC}}$ (mN·m <sup>-1</sup> )	pC <sub>20</sub>	CMC/C <sub>20</sub>	$\Gamma_{\text{max}}$ (10 <sup>-10</sup> mol·cm <sup>-2</sup> )	A <sub>min</sub> (nm <sup>2</sup> )	$\Delta G_{\text{m}}^{\theta}$ (kJ·mol <sup>-1</sup> )	$\Delta G_{\text{ads}}$ (kJ·mol <sup>-1</sup> )
a	5.08 × 10 <sup>-3</sup>	28.08	3.306	10.283	2.024	0.821	-23.05	-44.76
b	3.30 × 10 <sup>-4</sup>	26.11	4.465	9.621	2.278	0.730	-29.83	-50.00
c	1.55 × 10 <sup>-4</sup>	23.69	4.578	5.866	3.171	0.524	-31.70	-46.95
d	1.82 × 10 <sup>-4</sup>	24.90	4.770	10.717	2.361	0.704	-31.30	-51.27

Figure 2. Plots of conductivity ( $\kappa$ ) against the concentration ( $c$ ) of compounds a, b, c, and d at 298.15 K.

mN·m<sup>-1</sup>, lower than those of some reported quaternary ammonium surfactants, which are usually greater than 30 mN·m<sup>-1</sup>.<sup>26,27</sup> It indicates that these synthesized surfactants have higher surface activities. Table 1 also shows that the values of CMC and  $\gamma_{\text{CMC}}$  of these quaternary ammonium surfactants gradually decrease with increasing the alkyl chain length from 10 to 14 due to the enhanced hydrophobic interaction between the longer alkyl chains. However, as the alkyl chain length increases from 14 to 16, the values of CMC and  $\gamma_{\text{CMC}}$  increase. This may be because, with the further increase of the alkyl chain lengths, the aggregations of self-coiling or pre-micellar (such as dimer and trimer), which show little or no significant

surface activity, are formed at concentrations below the CMC.<sup>28,29</sup>

The maximum surface excess concentration ( $\Gamma_{\text{max}}$ ) and the minimum surface area ( $A_{\text{min}}$ ) of each surfactant molecule at the air–water interface are calculated using the Gibbs adsorption equation as following<sup>30</sup>

$$\Gamma_{\text{max}} = \left( \frac{-1}{nRT} \right) \left( \frac{d\gamma}{d \ln c} \right)_T = \left( \frac{-1}{2.303nRT} \right) \left( \frac{d\gamma}{d \log c} \right)_T \quad (1)$$

$$A_{\text{min}} = \frac{1}{N_A \Gamma_{\text{max}}} \quad (2)$$

In this article, we take the value  $n = 2$ .<sup>31</sup> The adsorption efficiency  $pC_{20}$  represents the negative logarithm of the surfactant concentration required to reduce the surface tension of pure water by  $20 \text{ mN}\cdot\text{m}^{-1}$ . The ratio of  $\text{CMC}/C_{20}$  reflects the tendency to form micelles relative to the tendency to adsorb at the air/water surface.<sup>32</sup> In addition, the Gibbs energy of adsorption ( $\Delta G_{\text{ads}}^\theta$ ) and the standard Gibbs free energy of micellization ( $\Delta G_{\text{m}}^\theta$ ) is calculated according to the Rosen method<sup>33</sup>

$$\Delta G_{\text{m}}^\theta = RT \ln \left( \frac{\text{CMC}}{55.5} \right) \quad (3)$$

$$\Delta G_{\text{ads}} = \Delta G_{\text{m}}^\theta - 6.023(\gamma_0 - \gamma_{\text{CMC}})A_{\text{min}} \quad (4)$$

The values of  $pC_{20}$ ,  $\text{CMC}/C_{20}$ ,  $\Gamma_{\text{max}}$ ,  $A_{\text{min}}$ ,  $\Delta G_{\text{m}}^\theta$ , and  $\Delta G_{\text{ads}}$  are also listed in Table 1.

As shown in Table 1, the values of  $\Gamma_{\text{max}}$  of these surfactants increase and the  $A_{\text{min}}$  values decrease with increasing the alkyl chain length from 10 to 14, indicating that the surfactant molecules with the longer hydrophobic chains pack more closely at the air–water interface due to a stronger interaction between the hydrocarbon chains. But, as the alkyl chain length increases from 14 to 16, there is an abnormal change in the values of  $\Gamma_{\text{max}}$  and  $A_{\text{min}}$ . A possible explanation is that the super long hydrophobic chain is more prone to bend at the air–water surface and makes compound d pack more loosely compared to compound c, resulting in the increase of the  $A_{\text{min}}$  value and the decrease of the  $\Gamma_{\text{max}}$  value.<sup>34</sup>

The  $pC_{20}$  values, used as a characterization of surfactant efficiency, increase with increasing the alkyl chain length, suggesting an increase in the efficiency of surfactant adsorption. The  $\text{CMC}/C_{20}$  ratio decreases with the increase of the hydrophobic alkyl chain length from 10 to 14, suggesting that the surfactant with a longer alkyl chain is more inclined to aggregate in a water phase and its adsorption is inhibited more than micellization.

In addition, all values found for  $\Delta G_{\text{ads}}$  and  $\Delta G_{\text{m}}^\theta$  are negative (Table 1), so it can be safely concluded that both adsorption and micellization of these surfactants are spontaneous at  $25^\circ\text{C}$ . Furthermore, the values of  $\Delta G_{\text{ads}}$  are more negative than those of  $\Delta G_{\text{m}}^\theta$ , which indicates that the adsorption of these surfactant systems is probably preferential than micellization.<sup>27</sup>

**3.4. Thermodynamic Properties of Micellization.** To further study the micellization behavior of these surfactants in aqueous solution, the conductivity was measured. Figure 2 demonstrates the plots of the conductivity ( $\kappa$ ) versus the concentration ( $c$ ) for compounds a–d at 298.15 K. As shown in Figure 2, the CMC values of the surfactants are determined by the sharp break points in the plots of  $\kappa$  versus  $c$ .<sup>35</sup> The degree of counterion dissociation ( $\alpha$ ) is determined from the ratio of slopes of the linear portions after and before the break point at CMC.<sup>36</sup> The degree of counterion binding ( $\beta$ ) equals  $1 - \alpha$ .  $\Delta G_{\text{m}}^\theta$  is calculated by the following equation<sup>37</sup>

$$\Delta G_{\text{m}}^\theta = RT \left( \frac{1}{2} + \beta \right) \ln x_{\text{CMC}} - \frac{1}{2} RT \ln 2 \quad (5)$$

In the equation,  $x_{\text{CMC}}$  is the unit mole fraction of the surfactants in the liquid phase at CMC, which can be approximated by  $\text{CMC}/55.5$ , where 55.5 represents the number of moles per liter of water at 298.15 K, and CMC is the values determined by the conductivity method. The values of CMC,  $\beta$ , and  $\Delta G_{\text{m}}^\theta$  are listed in Table 2.

**Table 2. Parameters of the Micellization of Compounds a, b, c, and d at 298.15 K**

compound	CMC ( $\text{mol}\cdot\text{L}^{-1}$ )	$\beta$	$\Delta G_{\text{m}}^\theta$ ( $\text{kJ}\cdot\text{mol}^{-1}$ )
a	$5.26 \times 10^{-3}$	0.467	−23.15
b	$3.51 \times 10^{-4}$	0.453	−29.28
c	$1.59 \times 10^{-4}$	0.438	−30.57
d	$1.64 \times 10^{-4}$	0.415	−29.56

As shown in Tables 1 and 2, the CMC values of the four surfactants determined by the conductivity method are very close to those found by the surface tension method. The results also show that the values of CMC obtained by the two methods follow the similar trend. Moreover, there is also an excellent agreement among the  $\Delta G_{\text{m}}^\theta$  values obtained by the two methods. In addition, it is obvious that the  $\beta$  values decrease with increasing the alkyl chain length. This can be attributed to the decrease in surface charge density of the micelles. Surfactants with longer alkyl chains are conducive to aggregation in bulky structures, in which the ratio of surface to volume is relatively smaller. It means that the polar head groups are packed more tightly and bound by more counterions.<sup>26</sup>

**3.5. Microenvironment and Aggregation.** The shape and intensity for the photoluminescence spectra of pyrene, especially the fluorescence intensity ratio  $I_1/I_3$ , are very sensitive to its microenvironment at the site of fluorophore solubilization. So, fluorescence spectroscopy is a useful and convenient technique for studying the micropolarity of surfactant aggregates. The variations of the pyrene polarity ratio  $I_1/I_3$  with the change of the surfactant concentration ( $c$ ) are shown in Figure 3. The CMC values of the surfactants,

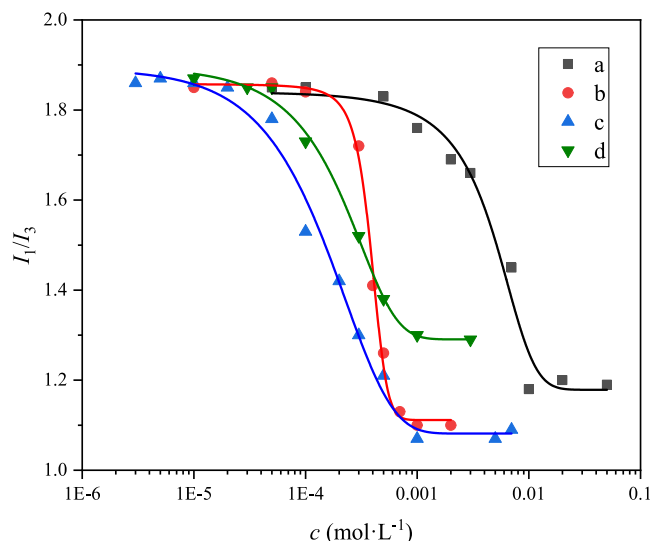


**Figure 3.** Variation of the pyrene fluorescence intensity ratio  $I_1/I_3$  with the surfactant concentration ( $c$ ) for compounds a, b, c, and d.

which are listed in Table 3, are determined by the center between initial and final horizontal asymptotes of the sigmoidal curve.<sup>38</sup> From Tables 1–3, we can see that the CMC values obtained by surface tension, conductivity, and steady-state fluorescence methods are very consistent.

As shown in Figure 3, when the surfactant concentration is low, the  $I_1/I_3$  ratio maintains in a high value and changes slightly, suggesting that pyrene has no interaction with the

**Table 3. Parameters of the Micellization of Compounds a, b, c, and d at 298.15**

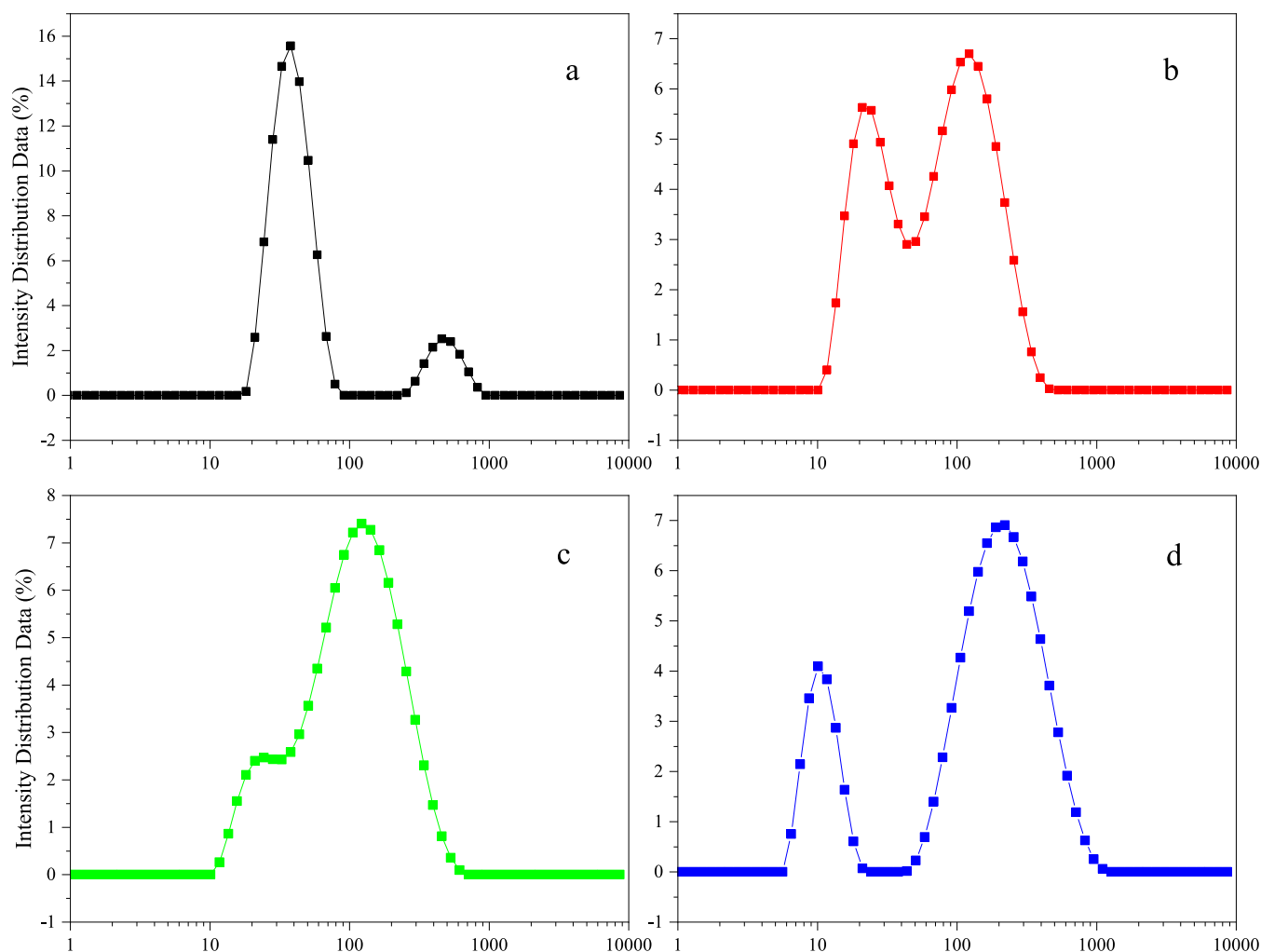
compound	CMC (mol·L <sup>-1</sup> )	$I_1/I_3$
a	$4.88 \times 10^{-3}$	1.18
b	$3.80 \times 10^{-4}$	1.10
c	$1.73 \times 10^{-4}$	1.07
d	$2.32 \times 10^{-4}$	1.29

surfactant at the outset. With increasing the surfactant concentration, the  $I_1/I_3$  ratio decreases rapidly, indicating that the pyrene is sensing a more hydrophobic environment due to the formation of micelles. Then, the  $I_1/I_3$  ratio reaches a roughly constant value, suggesting that the aggregate structures are compact and the microenvironment does not change. The  $I_1/I_3$  ratios at final horizontal asymptotes of the curves, which reflect the final micropolarity of the surfactant aggregates, are also listed in Table 3. As shown in Table 3, the  $I_1/I_3$  ratio of these surfactants is low, indicating that the pyrene is solubilized in the palisade layer near the polar head groups.<sup>39</sup> Table 3 also shows that the  $I_1/I_3$  ratios of these surfactants decrease from 1.18 to 1.07 as the alkyl chain length increases from 10 to 14, suggesting that the stronger hydrophobic interaction of the surfactants with longer alkyl chains leads to tighter aggregation in aqueous solutions and provides a more hydrophobic

microenvironment. However, the  $I_1/I_3$  ratio changes abnormally as the alkyl chain length increases from 14 to 16. One possible reason is that the super long hydrocarbon chain of the surfactant is more likely to curl up and forms looser aggregates, thus leading to the entrance of water molecules and resulting in a weaker hydrophobic microenvironment.<sup>34</sup>

**3.6.  $R_h$  Distributions and Morphology of the Aggregates.** The size and distribution of aggregates formed by these surfactants in SMC aqueous solution were examined by DLS (Figure 4). It is obvious that  $R_h$  distributions of these surfactants appear double peaks and are closed with each other, which are between 10 and 1000 nm. Furthermore, with the increase of the carbon chain length,  $R_h$  distributions of these surfactants in the range of 10–1000 nm have a little backward trend, that is, they tend to form aggregates with larger particle sizes. According to the DLS measurement results, these surfactant molecules form different aggregate types in aqueous solution, and the average  $R_h$  of the aggregates is 10–40 and 100–400 nm. This may be because the amide group in the surfactant molecular structure is prone to form intermolecular hydrogen bonds, which promotes molecular aggregation and forms different aggregate types.<sup>40</sup>

Correspondingly, the morphologies of aggregates of these surfactants in an aqueous solution of SMC are further carried out on TEM measurement, which are shown in Figure 5. It can

**Figure 4.**  $R_h$  distribution of compounds a, b, c, and d in aqueous solution with a concentration of SMC.

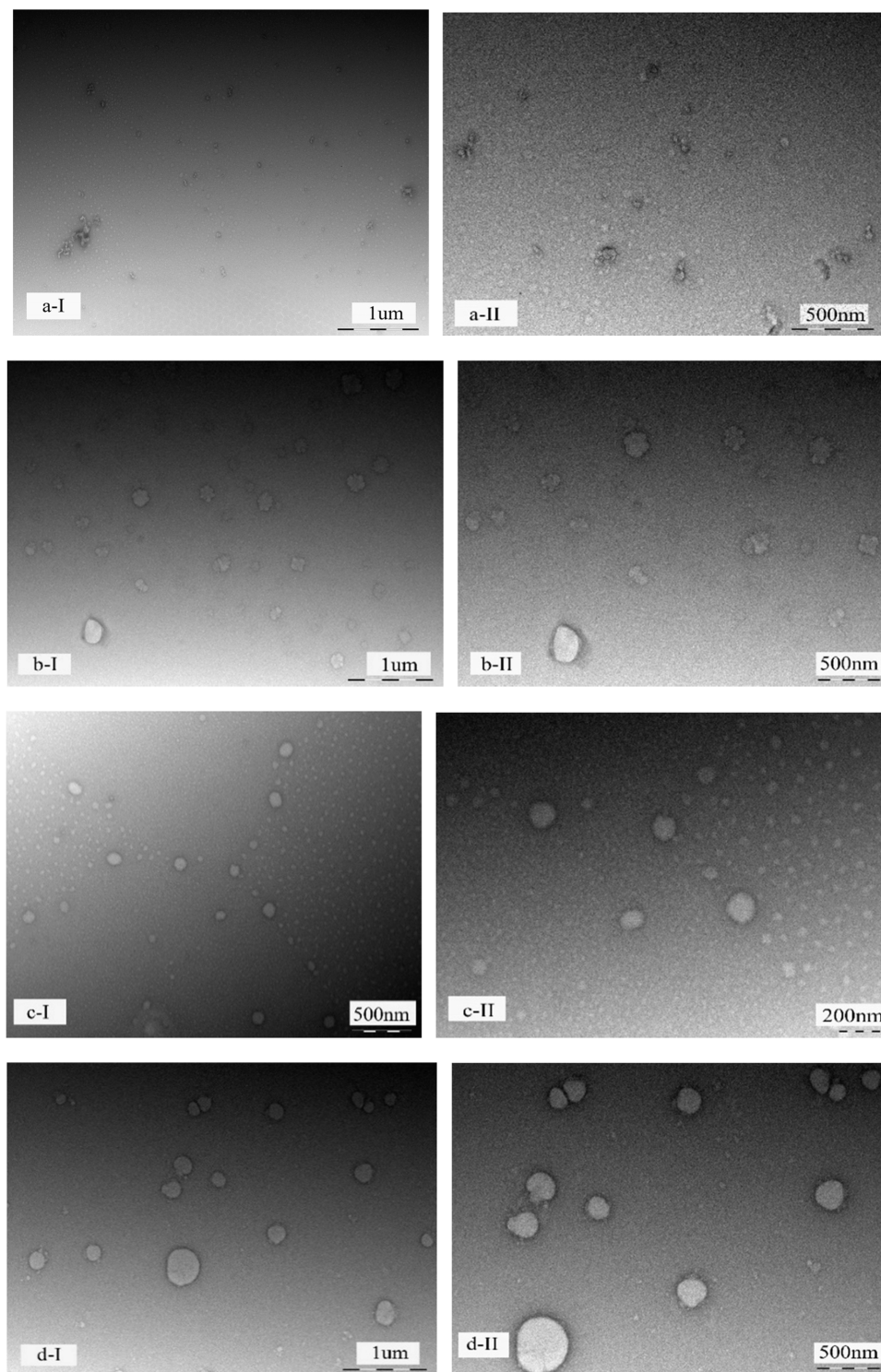


**Figure 5.** TEM micrographs of aggregates of compounds a, b, c, and d in aqueous solutions with a concentration of SCMC.

be found that spherical vesicles with different sizes are formed in surfactant aqueous solutions. The size (inner diameter) of the vesicles ranges 10–400 nm, which is basically consistent with the results of DLS. Because we cannot measure the thickness of the vesicle wall, it is difficult to confirm if they are monolayer or multilayer vesicles. The formation of vesicles may be due to the presence of amide groups in the molecular structure, which are prone to form intermolecular hydrogen bonds and promote the aggregation of rigid bilayer

structures.<sup>41</sup> The hydrogen bonding interactions near the head group region can minimize the repulsive interactions among the cationic  $N^+$  groups, thus favoring vesicle formation.<sup>42</sup>

**3.7. Foam Properties.** Figure 6 presents the foam properties of these amide quaternary ammonium surfactants and LAS. Figure 6A shows that the foam ability of the four surfactants and LAS increases gradually with increasing the temperature from 25 to 45 °C. It is thought that the Brownian

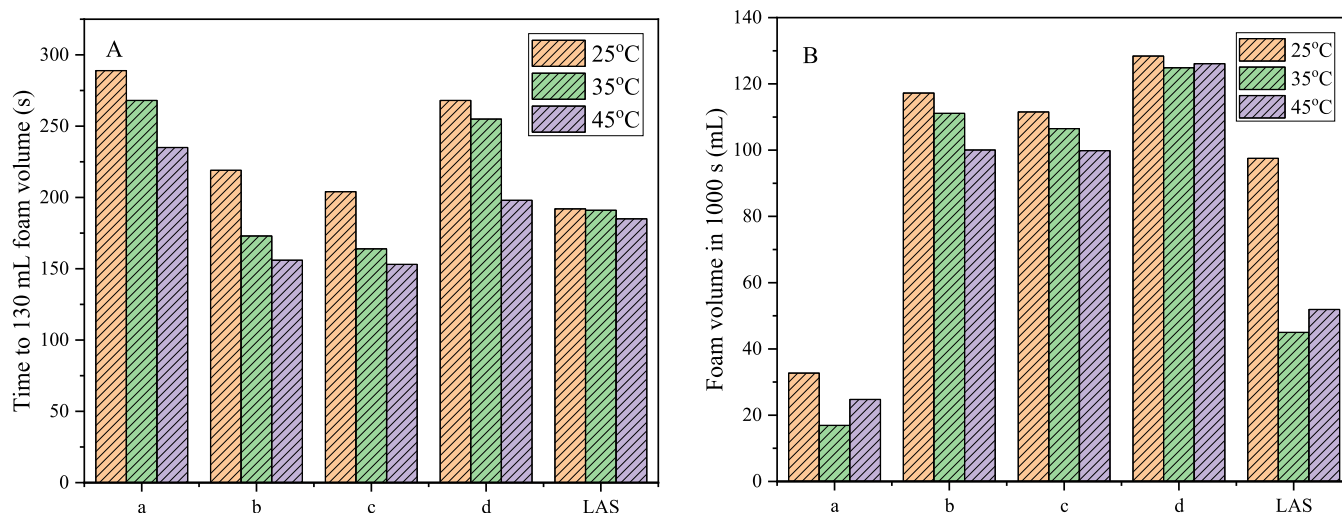


**Figure 6.** Foam ability (A) and foam stability (B) of compounds a, b, c, d, and LAS.

motion is the main reason for this phenomenon. In the Brownian motion, the kinematic velocity of the ions increases with the increase of temperature and leads to more frequent collisions between the ions, thereby increasing the foam ability.<sup>43</sup> From Figure 6A, we can also see that, with the increase of the carbon chain length, the foam ability of the four surfactants increases and then decreases at the same temperature, which is in contrast to the change trend of their  $\gamma_{\text{CMC}}$ . This may be because the surfactant solution with a low surface tension forms a thick liquid film, which is conducive to the formation of foam.<sup>44</sup> A comparison of the data in Figure 6 also shows that the time required for compounds b and c to generate 130 mL of foam is shorter than LAS at 35 and 45 °C, which means that compounds b and c are more prone to foam than LAS. From Figure 6B, we can also safely conclude that the foam stability of the four amide quaternary ammonium surfactants is best at 25 °C. The results can be explained as follows: at lower temperature, the gas diffusion rate, which peaks at 20–30 °C, may influence the foam stability, while with the increase of the temperature, the surface viscosity is thought to be the main influence, resulting in faster and faster liquid discharge. Thus, the foam stability is relatively lower at higher temperatures.<sup>43</sup> Figure 6B also shows that, at the same temperature, compound d exhibits the best foam stability, followed by b, c, and a, and the foam stability of compounds b, c, and d is better than that of LAS. It can be interpreted from the following aspects. The foam stability is relative to the surface viscosity of the liquid film. The interface configuration of the surfactant with a low surface tension and long hydrophobic carbon chain is more compact, which increases the strength of the liquid film, thus preventing the liquid from coming out of the liquid film, delaying the foam crumbling, and improving the stability of foam.<sup>45</sup>

#### 4. CONCLUSIONS

In this work, four amide quaternary ammonium surfactants, which possess excellent surface activities, are synthesized using a green reagent DMC. Studies have shown that, with increasing the alkyl chain length from 10 to 14, the values of CMC,  $\gamma_{\text{CMC}}$ , and  $A_{\text{min}}$  decrease, and the  $\Gamma_{\text{max}}$  values increase, indicating that the surfactant molecules with longer hydrophobic chains have higher efficiency and pack more closely at the air–water interface, while with an increase of the alkyl chain from 14 to

16, there is an abnormal change in these four values, probably due to the occurrence of self-coiling or the formation of pre-micellar aggregates. Furthermore, the  $\Delta G_{\text{ads}}$  values are more negative than those of  $\Delta G_{\text{m}}^{\theta}$ , suggesting that the adsorption of these surfactant systems is probably preferential than micellization. It is concluded from the  $\beta$  values that the increase of the chain length reduces the surface charge density of aggregates and weakens the electrostatic attractions between head groups and counterions. DLS and TEM results indicate that these synthesized surfactants self-assemble spontaneously into the aggregates with  $R_{\text{h}}$  distributions of 10–1000 nm, which are mostly vesicles. These surfactants are also found to exhibit excellent foam ability and foam stability.

#### ■ ASSOCIATED CONTENT

##### Supporting Information

The Supporting Information is available free of charge at <https://pubs.acs.org/doi/10.1021/acsomega.2c06353>.

Details of the spectral characterizations of compounds a–d; MS, <sup>1</sup>H NMR, <sup>13</sup>C NMR, and FTIR spectra of compounds a–d; plots of conductivity ( $\kappa$ ) against temperature; explanation of eqs 1 and 2; fluorescence spectra; polydispersity parameters; plots of foam height against time (PDF)

#### ■ AUTHOR INFORMATION

##### Corresponding Author

Hongqin Liu – School of Light Industry, Beijing Key Laboratory of Flavor Chemistry, Beijing Higher Institution Engineering Research Center of Food Additives and Ingredients, Beijing Technology and Business University, Beijing 100048, People's Republic of China; [orcid.org/0000-0003-2051-0342](https://orcid.org/0000-0003-2051-0342); Email: liuhongqin@th.btbu.edu.cn

##### Authors

Xinru Jia – School of Light Industry, Beijing Key Laboratory of Flavor Chemistry, Beijing Higher Institution Engineering Research Center of Food Additives and Ingredients, Beijing Technology and Business University, Beijing 100048, People's Republic of China

Ran Wei – School of Light Industry, Beijing Key Laboratory of Flavor Chemistry, Beijing Higher Institution Engineering

Research Center of Food Additives and Ingredients, Beijing Technology and Business University, Beijing 100048, People's Republic of China

Bo Xu – McIntire School of Commerce, University of Virginia, Charlottesville, Virginia 22903, United States

Bao-Cai Xu – School of Light Industry, Beijing Key Laboratory of Flavor Chemistry, Beijing Higher Institution Engineering Research Center of Food Additives and Ingredients, Beijing Technology and Business University, Beijing 100048, People's Republic of China

Complete contact information is available at:

<https://pubs.acs.org/10.1021/acsomega.2c06353>

## Notes

The authors declare no competing financial interest.

## ACKNOWLEDGMENTS

The work was supported by the National Key R&D Program of China (2017YFB0308701), the National Natural Science Foundation of China (21676003), and the Beijing Municipal Science and Technology Project (Z171100001317015).

## REFERENCES

- (1) Deleu, M.; Paquot, M. From Renewable Vegetables Resources to Microorganisms: New Trends in Surfactants. *C. R. Chim.* **2004**, *7*, 641–646.
- (2) Tezel, U.; Pavlostathis, S. G. Quaternary Ammonium Disinfectants: Microbial Adaptation, Degradation and Ecology. *Curr. Opin. Biotechnol.* **2015**, *33*, 296–304.
- (3) Mechken, K. A.; Menouar, M.; Belkhdja, M.; Saidi-Besbes, S. Synthesis, Surface Properties and Bioactivity of Novel 4-Substituted 1,2,3-Triazole Quaternary Ammonium Surfactants. *J. Mol. Liq.* **2021**, *338*, No. 116775.
- (4) zelechowski, K.; Gucma, M.; Golebiewski, W. M.; Krawczyk, M.; Michalczyk, A. K. Synthesis of New Quaternary Ammonium Salts with a Terpene Function and Evaluation of their Fungicidal and Herbicidal Activities. *Acta Chim. Slov.* **2020**, *67*, 325–335.
- (5) Kwaśniewska, D.; Chen, Y. L.; Wiczorek, D. Biological Activity of Quaternary Ammonium Salts and Their Derivatives. *Pathogens* **2020**, *9*, 459.
- (6) Jennings, M. C.; Minbiole, K. P. C.; Wuest, W. M. Quaternary Ammonium Compounds: an Antimicrobial Mainstay and Platform for Innovation to Address Bacterial Resistance. *ACS Infect. Dis.* **2015**, *1*, 288–303.
- (7) Brycki, B.; Koziróg, A.; Kowalczyk, I.; Pospieszny, T.; Materna, P.; Marciniak, J. Synthesis, Structure, Surface and Antimicrobial Properties of New Oligomeric Quaternary Ammonium Salts with Aromatic Spacers. *Molecules* **2017**, *22*, 1810.
- (8) Olkowska, E.; Polkowska, Z.; Namieśnik, J. Analytics of Surfactants in the Environment: Problems and Challenges. *Chem. Rev.* **2011**, *111*, 5667–5700.
- (9) He, X.; Wang, L.; Wu, J.; Yang, J.; Ma, W.; Bai, L.; Zhao, B.; Song, B. The Effects of Amide Bonds and Aromatic Rings on the Surface Properties and Antimicrobial Activity of Cationic Surfactants. *J. Surfactants Deterg.* **2019**, *22*, 315–325.
- (10) Hoque, J.; Gonuguntla, S.; Yarlagadda, V.; Aswal, V. K.; Haldar, J. Effect of Amide Bonds on the Self-assembly of Gemini Surfactants. *Phys. Chem. Chem. Phys.* **2014**, *16*, 11279–11288.
- (11) Hoque, J.; Kumar, P.; Aswal, V. K.; Haldar, J. Aggregation Properties of Amide Bearing Cleavable Gemini Surfactants by Small Angle Neutron Scattering and Conductivity Studies. *J. Phys. Chem. B* **2012**, *116*, 9718–9726.
- (12) Stjern Dahl, M.; Holmberg, K. Synthesis, Stability, and Biodegradability Studies of a Surface-active Amide. *J. Surfactants Deterg.* **2005**, *8*, 331–336.
- (13) Zhi, L.; Shi, X.; Zhang, E.; Pan, Y.; Li, X.; Wang, H.; Liu, W. Synthesis and Properties of Stellate Lactosamide Quaternary Ammonium Surfactants. *Colloids Surf., A* **2021**, *628*, No. 127317.
- (14) Hao, J.; Qin, T.; Zhang, Y.; Li, Y.; Zhang, Y. Synthesis, Surface Properties and Antimicrobial Performance of Novel Gemini Pyridinium Surfactants. *Colloids Surf., B* **2019**, *181*, 814–821.
- (15) Zhao, X.; An, D.; Ye, Z. A Comprehensive Study on the Synthesis and Micellization of Disymmetric Gemini Imidazolium Surfactants. *J. Surfactants Deterg.* **2016**, *19*, 681–691.
- (16) Sharma, R.; Kamal, A.; Abdinejad, M.; Mahajan, R. K.; Kraatz, H. B. Advances in the Synthesis, Molecular Architectures and Potential Applications of Gemini Surfactants. *Adv. Colloid Interface Sci.* **2017**, *248*, 35–68.
- (17) Perinelli, D. R.; Petrelli, D.; Vitali, L. A.; Bonacucina, G.; Cespi, M.; Vllasaliu, D.; Giorgioni, G.; Palmieri, G. F. Quaternary Ammonium Leucine-Based Surfactants: The Effect of a Benzyl Group on Physicochemical Properties and Antimicrobial Activity. *Pharmaceutics* **2019**, *11*, 287.
- (18) Aricò, F.; Tundo, P. Dimethyl Carbonate as a Modern Green Reagent and Solvent. *Russ. Chem. Rev.* **2010**, *79*, 479–489.
- (19) Patraşcu, I.; Bildea, C. S.; Kiss, A. A. Novel Eco-efficient Reactive Distillation Process for Dimethyl Carbonate Production by Indirect Alcoholysis of Urea. *Front. Chem. Sci. Eng.* **2022**, *16*, 316–331.
- (20) Šarić, M.; Davies, B. J. V.; Schjodt, N. C.; Dahl, S.; Moses, P. G.; Escudero-Escribano, M.; Arenz, M.; Rossmesl, J. Catalyst Design Criteria and Fundamental Limitations in the Electrochemical Synthesis of Dimethyl Carbonate. *Green Chem.* **2019**, *21*, 6200–6209.
- (21) Mukherjee, P. Green Chemistry-A Novel Approach Towards Sustainability. *J. Chil. Chem. Soc.* **2021**, *66*, 5075–5080.
- (22) Liu, S.; Wang, X.; Chen, L.; Hou, L.; Zhou, T. Aggregation Morphologies of a Series of Heterogemini Surfactants with a Hydroxyl Head Group in Aqueous Solution. *Soft Matter* **2014**, *10*, 9177–9186.
- (23) Tanaka, A.; Ikeda, S. Adsorption of Dodecyltrimethyl Ammonium Bromide on Aqueous Surfaces of Sodium Bromide Solutions. *Colloids Surf.* **1991**, *56*, 217–228.
- (24) Zhang, C.; Jiang, Y.; Ju, H.; Wang, Y.; Geng, T. “Organic Counterion” Modified Quaternary Ammonium Salt: Impact on Antibacterial Activity & Application Properties. *J. Mol. Liq.* **2017**, *241*, 638–645.
- (25) Manet, S.; Karpichev, Y.; Bassani, D.; Kiagus-Ahmad, R.; Oda, R. Counteranion Effect on Micellization of Cationic Gemini Surfactants 14-2-14: Hofmeister and Other Counterions. *Langmuir* **2010**, *26*, 10645–10656.
- (26) Asadov, Z. H.; Ahmadova, G. A.; Rahimov, R. A.; Abilova, A. Z.; Zargarova, S. H.; Zubkov, F. I. Synthesis and Properties of Quaternary Ammonium Surfactants Based on Alkylamine, Propylene Oxide, and 2-Chloroethanol. *J. Surfactants Deterg.* **2018**, *21*, 247–254.
- (27) Xu, D.; Ni, X.; Zhang, C.; Mao, J.; Song, C. Synthesis and Properties of Biodegradable Cationic Gemini Surfactants with Diester and Flexible Spacers. *J. Mol. Liq.* **2017**, *240*, 542–548.
- (28) Yoshimura, T.; Ishihara, K.; Esumi, K. Sugar-based Gemini Surfactants with Peptide Bonds-synthesis, Adsorption, Micellization, and Biodegradability. *Langmuir* **2005**, *21*, 10409–10415.
- (29) Bordi, F.; Cerichelli, G.; de Berardinis, N.; Diociaiuti, M.; Giansanti, L.; Mancini, G.; Sennato, S. Synthesis and Physicochemical Characterization of New Twin-tailed N-oxide Based Gemini Surfactants N-oxide Based Gemini Surfactants. *Langmuir* **2010**, *26*, 6177–6183.
- (30) Kamboj, R.; Singh, S.; Chauhan, V. Synthesis, Characterization and Surface Properties of N-(2-hydroxyalkyl)-N'-(2-hydroxyethyl) Imidazolium Surfactants. *Colloids Surf., A* **2014**, *441*, 233–241.
- (31) Tawfik, S. M. Synthesis, Surface, Biological Activity and Mixed Micellar Phase Properties of some Biodegradable Gemini Cationic Surfactants Containing Oxycarbonyl Groups in the Lipophilic Part. *J. Ind. Eng. Chem.* **2015**, *28*, 171–183.
- (32) Tsubone, K.; Arakawa, Y.; Rosen, M. J. Structural Effects on Surface and Micellar Properties of Alkanediyl- $\alpha$ ,  $\omega$ -bis (sodium N-

- acyl- $\beta$ -alaninate) Gemini Surfactants. *J. Colloid Interface Sci.* **2003**, *262*, 516–524.
- (33) Rosen, M. J.; Kunjappu, T. J. *Surfactants and Interfacial Phenomena*, 4th ed.; Wiley: New York, 2012.
- (34) Zhou, L.; Jiang, X.; Li, Y.; Chen, Z.; Hu, X. Synthesis and Properties of a Novel Class of Gemini Pyridinium Surfactants. *Langmuir* **2007**, *23*, 11404.
- (35) Fatma, N.; Panda, M.; Ansari, W. H.; Kabir-ud-Din. Environment-Friendly Ester Bonded Gemini Surfactant: Mixed Micellization of 14-E2-14 with Ionic and Nonionic Conventional Surfactants. *J. Mol. Liq.* **2015**, *211*, 247–255.
- (36) Zana, R.; Benrraou, M.; Rueff, R. Alkanediyl- $\alpha$ ,  $\omega$ -bis-(dimethyl alkyl ammonium bromide) Surfactants. 1. Effect of the Spacer Chain Length on the Critical Micelle Concentration and Micelle Ionization Degree. *Langmuir* **1991**, *7*, 1072–1075.
- (37) Zana, R. Critical Micellization Concentration of Surfactants in Aqueous Solution and Free Energy of Micellization. *Langmuir* **1996**, *12*, 1208–1211.
- (38) Liu, H. Q.; Zhou, X. Q.; Zhang, X. X.; Shi, G. Y.; Hu, J.; Liu, C. Y.; Xu, B. C. Green Synthesis, Surface Activity, Micellar Aggregation, and Corrosion Inhibition Properties of New Gemini Quaternary Ammonium Surfactants. *J. Chem. Eng. Data* **2018**, *63*, 1304–1315.
- (39) Ao, M. Q.; Huang, P. P.; Xu, G. Y.; Yang, X. D.; Wang, Y. J. Aggregation and Thermodynamic Properties of Ionic Liquid-type Gemini Imidazolium Surfactants with Different Spacer Length. *Colloid Polym. Sci.* **2009**, *287*, 395–402.
- (40) Wang, L.; Yang, J.; He, X.; et al. Study on the Surface Properties and Aggregation Behavior of Quaternary Ammonium Surfactants with Amide Bonds. *ACS Omega* **2020**, *5*, 17042–17050.
- (41) Bajani, D.; Gharai, D.; Dey, J. A Comparison of the Self-assembly Behaviour of Sodium N-lauroyl Sarcosinate and Sodium N-lauroyl Glycinate Surfactants in Aqueous and Aqueo-organic Media. *J. Colloid Interface Sci.* **2018**, *529*, 314–324.
- (42) Bao, Y.; Guo, J.; Ma, J.; et al. Cationic Silicon-based Gemini Surfactants: Effect of Hydrophobic Chains on Surface Activity, Physico-chemical Properties and Aggregation Behaviors. *J. Ind. Eng. Chem.* **2017**, *53*, 51–61.
- (43) Wang, H. T.; Guo, W. B.; Zheng, C. B.; Wang, D. M.; Zhan, H. H. Effect of Temperature on Foaming Ability and Foam Stability of Typical Surfactants Used for Foaming Agent. *J. Surfactants Deterg.* **2017**, *20*, 615–622.
- (44) Xu, Y. M.; Zhang, X. X.; Zhao, H. X.; Chen, W.; Yan, X. D.; Liu, H. Q.; Liu, C. Y.; Xu, B. C. Synthesis, Characterization, and Surface-Active Properties of Carboxyl- betaine and Sulfobetaine Surfactants based on Vegetable Oil. *J. Surfactants Deterg.* **2017**, *20*, 615–622.
- (45) Chen, C. L.; Liao, Y. F.; Lu, F.; Zheng, Y. S.; Peng, Y. Y.; Ding, C. W.; Tong, Q. X. Facile Synthesis, Surface Activity, Wettability and Ultrahigh Foaming Properties of Novel Nonionic Gemini Fluoro-carbon Surfactants. *J. Mol. Liq.* **2020**, *302*, No. 112469.